

Gene correction of *HAX1* reversed Kostmann disease phenotype in patient-specific induced pluripotent stem cells

Erik Pittermann,^{1,2} Nico Lachmann,^{2,3} Glenn MacLean,^{4,5} Stephan Emmrich,¹ Mania Ackermann,^{2,3} Gudrun Göhring,^{2,6} Brigitte Schlegelberger,^{2,6} Karl Welte,⁷ Axel Schambach,^{2,3} Dirk Heckl,¹ Stuart H. Orkin,^{4,5,8} Tobias Cantz,^{2,9,*} and Jan-Henning Klusmann^{1,*}

¹Department of Pediatric Hematology and Oncology, ²Cluster of Excellence REBIRTH, and ³Institute of Experimental Hematology, Hannover Medical School, Hannover, Germany; ⁴Division of Hematology/Oncology, Boston Children's Hospital, Boston, MA; ⁵Department of Pediatric Oncology, Dana-Farber Cancer Institute, Boston, MA; ⁶Department of Human Genetics, Hannover Medical School, Hannover, Germany; ⁷Department of Hematology, Oncology and Bone Marrow Transplantation, Children's Hospital, University Hospital Tübingen, Tübingen, Germany; ⁸Howard Hughes Medical Institute, Harvard Medical School, Boston, MA; and ⁹Department of Gastroenterology, Hepatology, and Endocrinology, Hannover Medical School, Hannover, Germany

Key Points

- *HAX1*^{W44X}-iPSCs recapitulate Kostmann disease phenotype in vitro.
- Genetic in situ correction of iPSCs reveals a dysregulated *HAX1* and *HCLS1*-centered interaction network in Kostmann disease.

Severe congenital neutropenia (SCN, Kostmann disease) is a heritable disorder characterized by a granulocytic maturation arrest. Biallelic mutations in *HCLS1 associated protein X-1 (HAX1)* are frequently detected in affected individuals, including those of the original pedigree described by Kostmann in 1956. To date, no faithful animal model has been established to study SCN mediated by *HAX1* deficiency. Here we demonstrate defective neutrophilic differentiation and compensatory monocyte overproduction from patient-derived induced pluripotent stem cells (iPSCs) carrying the homozygous *HAX1*^{W44X} nonsense mutation. Targeted correction of the *HAX1* mutation using the CRISPR-Cas9 system and homologous recombination rescued neutrophil differentiation and reestablished an *HAX1* and *HCLS1*-centered transcription network in immature myeloid progenitors, which is involved in the regulation of apoptosis, apoptotic mitochondrial changes, and myeloid differentiation. These findings made in isogenic iPSC-derived myeloid cells highlight the complex transcriptional changes underlying Kostmann disease. Thus, we show that patient-derived *HAX1*^{W44X}-iPSCs recapitulate the Kostmann disease phenotype in vitro and confirm *HAX1* mutations as the disease-causing monogenic lesion. Finally, our study paves the way for nonvirus-based gene therapy approaches in SCN.

Introduction

Severe congenital neutropenia (SCN) represents a rare hematologic disease entity that is clinically characterized by an absolute neutrophil count $<0.5 \times 10^9/L$ because of a granulocytic differentiation arrest at the promyelocyte stage.¹ Patients may develop life-threatening bacterial infections if not treated with recombinant granulocyte colony-stimulating factor (G-CSF) to elevate neutrophil blood counts.¹ Rolf Kostmann first characterized the disease in Swedish patients in 1956 as infantile genetic agranulocytosis.² Multiple hereditary mutations have been reported in different forms of SCN (eg, in *ELA2*, *G6PC3*, *GFI1*, *WASP*, *SLC37A4*).³ Autosomal recessive mutations in *HCLS1-associated protein X-1 (HAX1)* were reported in 2007 as the genetic defect in the original Kostmann patients and many other families.^{4,5}

Although the clinical phenotype of Kostmann disease is well-characterized, the pathogenesis is incompletely understood. *HAX1* is a ubiquitously expressed protein.⁵ Its subcellular localization in the mitochondrial membrane, endoplasmic reticulum, and cytoplasm⁶⁻⁸ suggest a role in several cellular processes. *HAX1*

Submitted 14 December 2016; accepted 2 April 2017. DOI 10.1182/bloodadvances.2016003798.

*T.C. and J.-H.K. contributed equally to this study.

The data reported in this article have been deposited in the Gene Expression Omnibus (accession number GSE97414).

The full-text version of this article contains a data supplement.

© 2017 by The American Society of Hematology

appears to be involved in antiapoptotic signaling through the activation of HTRA2 and the subsequent inhibition of mitochondrial outer membrane permeabilization by BAX accumulation.⁹ In addition, Skokowa et al suggested that HAX1, together with HCLS1, plays a role in Wnt/LEF1-mediated hematopoietic differentiation by transcriptional activation of CEBP α .¹⁰ However, *Hax1* homozygous-null mice (*Hax1*^{-/-}) have normal granulocyte counts in peripheral blood, but exhibit extensive apoptosis of neurons and lymphocytes and impaired B-cell development.¹¹ Loss of motor neuron functions caused postnatal lethality in <14 weeks; thus, *Hax1*^{-/-} mice do not model the phenotype of human Kostmann disease. As a result, preclinical research is limited to human in vitro disease models and formal proof for the *HAX1* mutations because the causative and monogenic event in Kostmann disease is lacking.

Induced pluripotent stem cell (iPSC) technology provides an efficient and versatile platform to study rare hematologic disorders in vitro¹²⁻¹⁴ and allows fulfillment of Koch's postulates in genetic diseases that cannot be recapitulated in animal models.¹⁵ Although a homozygous, 256C>T nonsense mutation in *HAX1* (*HAX1*^{R86X}) has been modeled previously using iPSCs,¹⁶ this variant has been described in only 2 patients and lies outside of exon 2a, the region where the majority of the reported mutations reside.⁴ Moreover, this variant has been linked to neurological deficits.^{4,17} In addition, viral-based overexpression of wild-type (WT) *HAX1* complementary DNA (cDNA) was applied to revert the granulocytic differentiation arrest compared with iPSCs derived from a healthy individual.¹⁶

Here, we investigated iPSC-derived granulopoiesis from Kostmann patients (*HAX1*^{W44X}-iPSCs) and gene-corrected isogenic lines generated by CRISPR-Cas9 gene editing. Using a new, robust neutrophilic differentiation assay, we have successfully modeled the Kostmann hematologic phenotype that is characterized by perturbed granulocytic differentiation and compensatory overproduction of monocytes.⁵ We demonstrate that targeted correction of the *HAX1* mutation reestablished a *HAX1*- and *HCLS1*-centered transcription network in immature myeloid progenitors, which is involved in the regulation of apoptosis and also myeloid differentiation. Finally, our study paves the way for nonvirus-based gene therapy approaches in SCN.

Methods and materials

Cell culture

All experiments done with human embryonic stem cells (ESCs) and human iPSCs were approved by the German federal authorities (Robert Koch Institute: Aktenzeichen: 1710-79-1-4-41-E01). H9 ESCs were obtained from WiCell Research Institute (Madison, WI). CF1 mouse embryonic fibroblasts were kindly provided by the Max Planck Institute for Molecular Biomedicine, Münster, Germany. WT iPSCs were obtained and derived as described.¹⁸ The patient-derived skin fibroblasts were obtained and provided by the Severe Chronic Neutropenia International Registry. Informed consent was obtained from all patients and/or custodians, after institutional review board approval, according to national law and regulations and in accordance to the Declaration of Helsinki. For virus production, 293T cells were used (CRL-3216; ATCC, Manassas, VA).

Reprogramming

The RRL.PPT.SF.hOct34.hKlf4.hSox2.i2dTomato.pre lentiviral vector was used for cellular reprogramming.¹⁹ To enhance reprogramming

efficiency, the microRNA 302/367 cluster was cloned into the backbone of the LeGO-G/BSD backbone (Addgene plasmid ID: 27354)²⁰ for cotransduction with *OCT4*, *KLF4*, and *SOX2*.

Targeted gene correction

The CRISPR-Cas9-based gene correction was done as described by Ran et al²¹ using the pX330 plasmid (Addgene plasmid ID: 42230)²² and a 90-nt single-stranded oligodeoxynucleotide ([ssODN] produced by IDT, Coralville, IA; supplemental Table 1) for homology-directed repair. The ssODN was centered on the *HAX1*^{W44X} mutation site. To test the cleavage efficiency of the targeting subgenomic RNA (sgRNA), a previously published reporter assay was used.²³

Karyotype analysis

Classical chromosome banding analysis was carried out by the Department of Human Genetics of Hannover Medical School. Description of chromosomal aberrations and clone definition followed the recommendations of the International System for Cytogenetic Nomenclature, 2013.

Neutrophilic differentiation of iPSCs

Neutrophilic differentiation was performed as recently described.²³ In short, iPSC colonies were detached as small fragments and shaken in suspension culture plates in basal embryonic stem cell medium at 100g for 5 days. Embryoid bodies were then collected and transferred to adherent culture plates in STEMdiff APEL medium (StemCell Technologies, Vancouver, BC, Canada) supplemented with 50 ng/mL G-CSF and 25 ng/mL interleukin-3 (Peprotech, Rocky Hill, NJ). Starting at day 15, suspension cells were collected and further cultured in RPMI 1640 supplemented with Glutamine (Merck Millipore), 10% fetal calf serum, and 50 ng/mL G-CSF for 7 to 14 days. Differentiated cells were then used for neutrophilic characterization.

Gene expression profiling

Isolated RNA samples of CD33⁺ myeloid progenitors were preamplified using Ovation RNA Amplification System V2 (Nugene, Irvine, CA). Expression profiles were generated on the Agilent SurePrint G3 platform in the Genome Analytics Department of Helmholtz Centre for Infection Research in Braunschweig, Germany. Expression data were analyzed with Genespring GX (Agilent, Santa Clara, CA), Gene Set Enrichment Analysis,²⁴ and g:Profiler.²⁵ Gene interaction networks were generated using GeneMANIA²⁶ and Cytoscape 3.4.²⁷

Results

Generation of Kostmann disease iPSCs

In 2007, Klein et al identified biallelic mutations in *HAX1* in Kostmann patients.⁵ To obtain disease-specific iPSCs, we reprogrammed skin fibroblasts of 1 patient from the original pedigree⁵ using Cre-excisable lentiviral vectors (supplemental Figure 1A-C). The patient carried the homozygous 130_131insA nonsense mutation in *HAX1* leading to a lack of WT *HAX1* protein expression from a premature stop codon (W44X).⁵ Sequencing of *HAX1* exon 2 confirmed that the 130_131insA mutation was retained on both alleles after reprogramming (Figure 1A). Morphology and alkaline phosphatase expression of *HAX1*^{W44X}-iPSCs were comparable to the H9 ESC control (Figure 1B). Quantitative reverse transcriptase polymerase chain reaction (RT-PCR) and immunocytochemistry confirmed the expression of the pluripotency genes *OCT4*, *SOX2*,

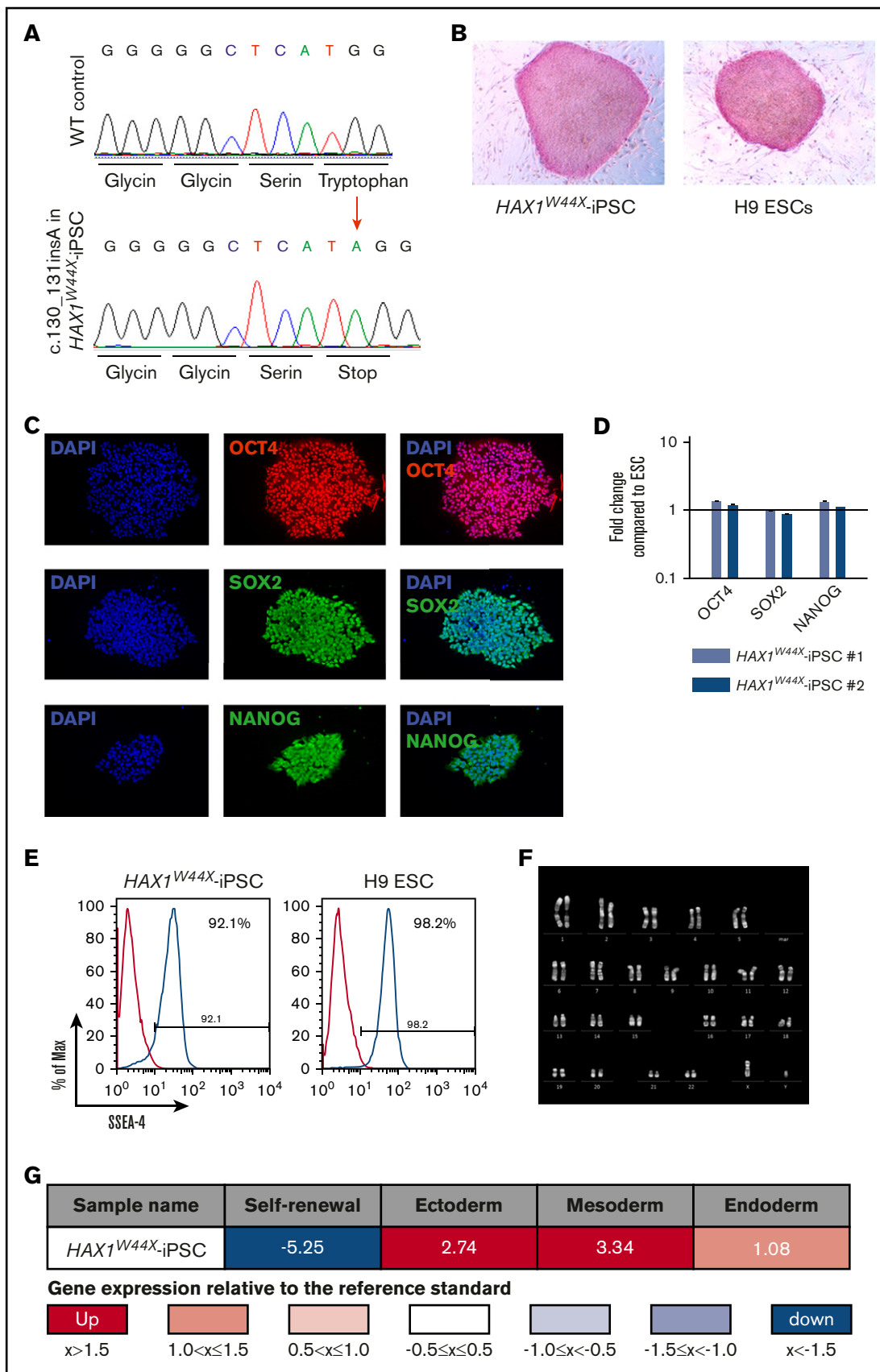


Figure 1.

and *NANOG* at the messenger RNA and protein level (Figure 1C-D). Pluripotency surface marker staining of SSEA-4 showed a similar expression pattern of *HAX1*^{W44X}-iPSCs and H9 ESCs (Figure 1E). No chromosomal aberrations were detected by karyotype analysis (Figure 1F). To functionally assess the quality of *HAX1*^{W44X}-iPSCs, differentiation potential into ectoderm, mesoderm, and endoderm was tested using the scorecard assay.²⁸ Following undirected differentiation, *HAX1*^{W44X}-iPSCs showed upregulation of genes of all germ layers, whereas pluripotency genes were strongly downregulated (Figure 1G; supplemental Figure 2). Therefore, we successfully generated *HAX1*^{W44X}-iPSCs from patient-derived skin fibroblasts.

Targeted correction of nonsense mutation in *HAX1*^{W44X}-iPSCs using CRISPR-Cas9-induced homology directed repair

To provide a specific and efficient correction of the mutation in Kostmann disease iPSCs, we used the CRISPR-Cas9 technology (Figure 2A).²¹ For homology-directed repair, we designed a 90-nt ssODN as the corrected donor sequence. A guide was selected that cleaves the genomic DNA 3 base pairs upstream of the mutation site. To avoid ssODN cleavage by Cas9, we introduced a silent mutation in the serine codon upstream of the correction site (Figure 2A). Using a restriction-based screening approach followed by Sanger sequencing, we successfully identified 2 corrected clones of the 288 that were tested (Figure 2B-D). Our biallelic homology-directed repair efficiency of 0.7% is in the range of reported frequencies.²⁹ Restoration of *HAX1* protein expression after genetic correction was confirmed by western blotting (Figure 2E). The expression level was comparable to that in the promyelocytic cell line NB-4.

To exclude chromosomal instability caused by CRISPR-Cas9 editing, karyotype analysis was performed after genetic correction, and no chromosomal aberrations were detected in either corrected clone (Figure 2F). Furthermore, the sequences of the top 5 off-target sites³⁰ that have 4 or more mismatches (*TMEM255A*, *SHISA7*, *MARK4*, *PTH2*, and *DST*; supplemental Table 2) showed no abnormalities when compared with its isogenic *HAX1*^{W44X}-iPSC clone (supplemental Figure 3). Taken together, gene correction using CRISPR-Cas9 technology rescued *HAX1* protein expression in *HAX1*^{W44X}-iPSCs.

Correction of mutated *HAX1* rescues Kostmann disease phenotype of patient-derived iPSCs

To assess the granulocytic differentiation potential of *HAX1*^{W44X} iPSCs and isogenic gene-corrected iPSCs (*HAX1*^{corrected}-iPSCs), a 2-step protocol was used (Figure 3A).²³ iPSCs from a healthy donor served as the WT control (*HAX1*^{WT/WT}-iPSC). The proliferation rates of *HAX1*^{W44X}-iPSCs, gene-corrected iPSCs (*HAX1*^{corrected}-iPSCs), and *HAX1*^{WT/WT}-iPSCs did not significantly differ (supplemental Figure 4). In the first step, embryoid bodies (EBs) were generated

from colony fragments. EBs were then seeded on attachment culture plates and incubated in hematopoietic specification medium containing interleukin-3 and G-CSF. In the second step, hematopoietic suspension cells were collected and further cultured in neutrophilic differentiation medium containing G-CSF. Using this protocol, granulocytes were derived from *HAX1*^{WT/WT}-iPSCs with a purity of 91% to 99% as quantified by morphology (Figure 3B-C). In contrast, we observed that *HAX1*^{W44X}-iPSCs predominantly differentiated into monocytes (Figure 3B-C), a finding consistent with the clinical phenotype.⁵ Few granulocytes (28%; range, 13% to 44%, $P < .01$) were present in *HAX1*^{W44X}-iPSC-derived cells (Figure 3B-C). Similar findings were observed in 2 additional *HAX1*^{W44X}-iPSC clones (data not shown). After targeted gene correction, differentiation of iPSCs yielded a highly enriched granulocytic cell population almost at the level of *HAX1*^{WT/WT}-iPSCs (91%; range, 83% to 99%; Figure 3B-C). By flow cytometry, CD11b⁺CD15⁺ neutrophilic cells reached a purity of 61% (range, 59% to 73%) in *HAX1*^{corrected} and 75% (range, 61% to 83%) in *HAX1*^{WT/WT}-iPSC clones, but only 28% (range, 21% to 35%) in the parental *HAX1*^{W44X} clone ($P < .01$; Figure 3D-E). To further validate the function of the generated neutrophils, cells were stimulated with phorbol 12-myristate 13-acetate (PMA) to form neutrophil extracellular traps (NETs, Figure 3F). In primary neutrophilic granulocytes from the peripheral blood of a healthy donor, DNA staining showed NETs consisting of typical weblike structures. *HAX1*^{W44X}-iPSC-derived cells did not form such NETs, whereas numerous NETs were observed in the corrected isogenic and the *HAX1*^{WT/WT} clones (Figure 3F). An immortalized T-cell line (Jurkat) was used as a negative control and showed no activation following PMA treatment.

Taken together, this set of data supports recapitulation of the Kostmann phenotype using in vitro differentiation of patient-derived iPSCs, which was reversed by targeted gene correction. *HAX1*^{corrected}-iPSCs yielded highly enriched neutrophilic populations that were able to form NETs upon PMA stimulation.

Genetic correction of *HAX1*^{W44X} reestablishes *HAX1*/*HCLS1*-centered gene expression network

To investigate the transcriptional changes consequent to mutated *HAX1*, we performed global gene expression profiling of SSC^{low}/CD33⁺ myeloid progenitors that were fluorescence-activated cell sorted after hematopoietic specification of the iPSC in vitro differentiation protocol (Figure 3A; supplemental Figure 5). We decided to use CD33⁺ myeloid progenitors for this analysis because the granulocytic differentiation arrest seen in Kostmann disease only becomes apparent after the promyelocyte stage. Comparison of *HAX1*^{W44X} with *HAX1*^{WT/WT} isogenic myeloid progenitors demonstrated the downregulation of a granulocyte expression program. Granulocyte-specific³¹ and myeloid-specific³² gene sets were negatively enriched (Figure 4A; supplemental Figure 6A, supplemental Table 3). Among the downregulated genes

Figure 1. Characterization of patient-derived *HAX1*^{W44X}-iPSC. Generated *HAX1*^{W44X}-iPSCs were compared with H9 ESCs and showed activation of their pluripotency network. (A) Sanger sequencing of *HAX1*^{W44X}-iPSCs confirmed the c.130_131insA mutation leading to a stop codon in exon 2 of *HAX1*. (B) High expression pattern of alkaline phosphatase in ESCs was also detectable in generated iPSCs. Original magnification $\times 100$; Naphthol/Fast Red Violet Solution. (C-D) Detection of pluripotency factors *OC74*, *SOX2*, and *NANOG* by (C) immunohistochemistry (original magnification $\times 200$) and (D) quantitative RT-PCR ($n = 3$, reference bar represents H9 ESC). (E) Flow cytometric quantification of ESC surface marker SSEA-4. (F) Karyotype analysis showed no chromosomal aberrations after reprogramming in *HAX1*^{W44X}-iPSCs. (G) Upon undirected EB-based differentiation, scorecard assays demonstrated the capability of generated iPSCs to differentiate in all 3 germ layers. Pluripotency genes were strongly downregulated. EB, embryoid body.

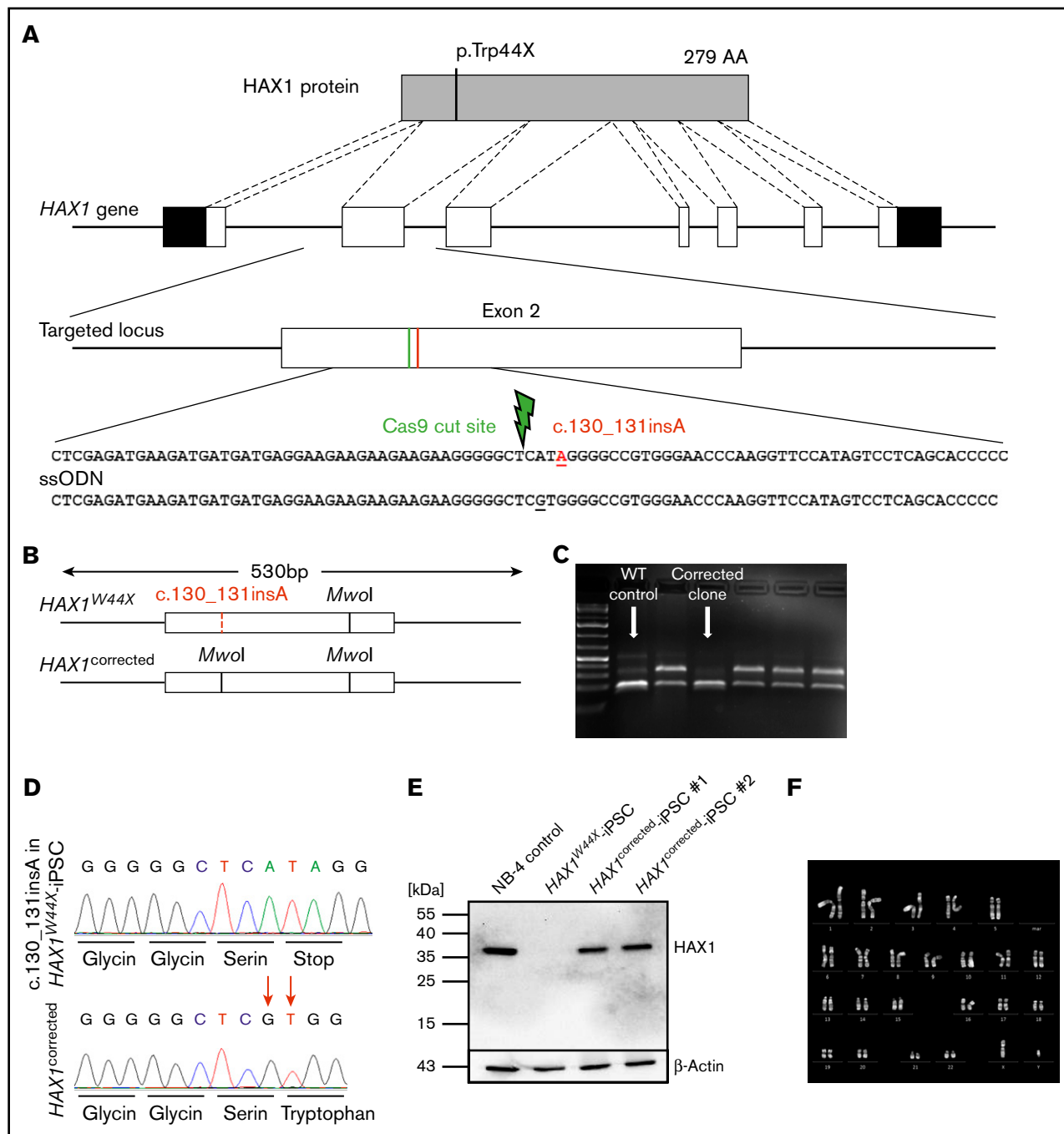


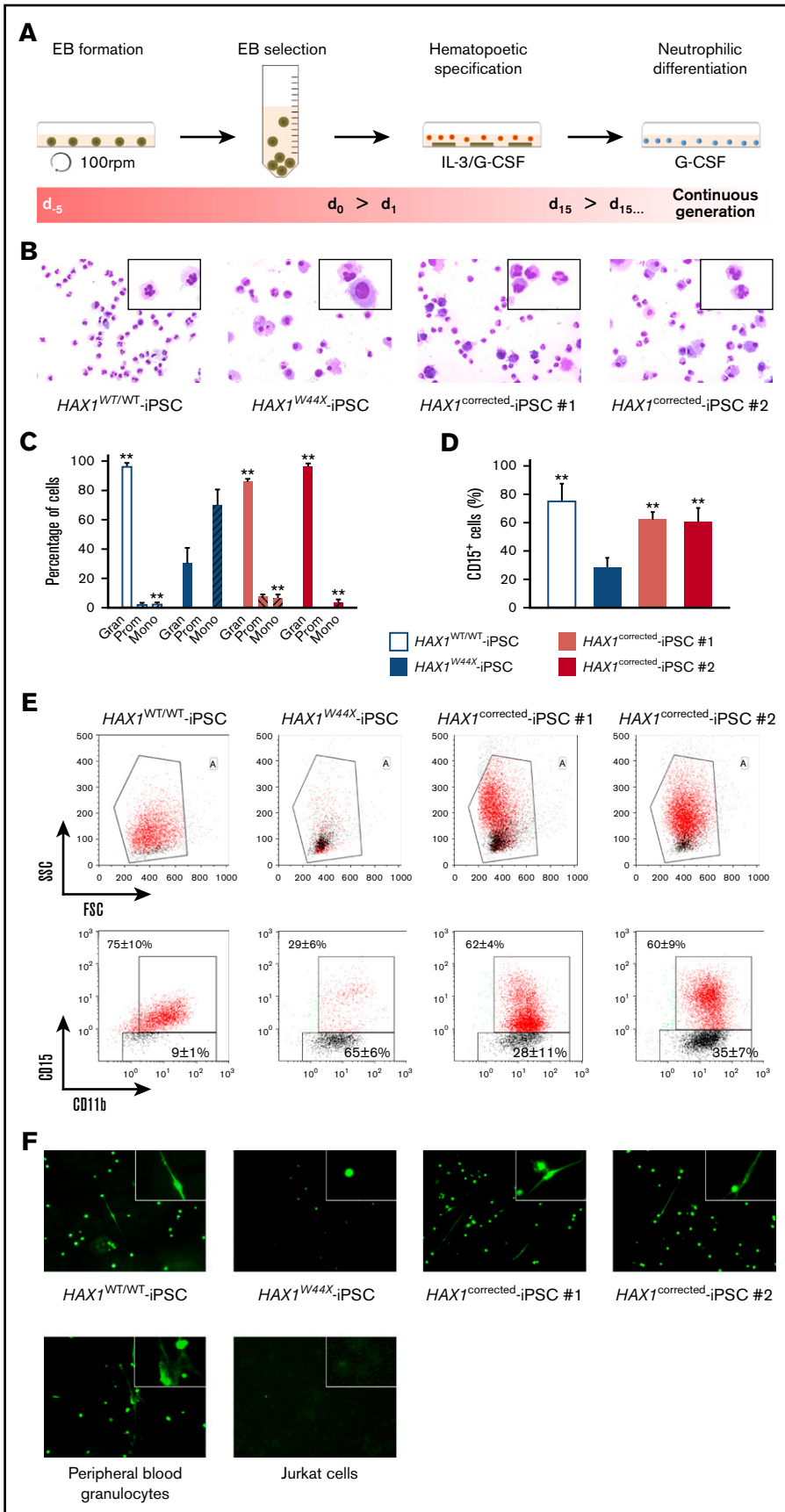
Figure 2. Targeted correction of c.130_131insA restored HAX1 protein expression. (A) Schematic overview of the HAX1 protein and the corresponding genomic locus including the location of c.130_131insA insertional mutation, which leads to a premature stop codon. The c.130_131insA mutation and the location of the double-strand break are indicated in red and green, respectively. The ssODN provided the corrected sequence and a silent mutation in the serine codon upstream of the mutation site. (B-C) Upon successful correction, a restriction site for *MwoI* was gained in exon 2 that was used to distinguish corrected clones from uncorrected after agarose gel electrophoresis (C). In corrected and WT clones, the additional *MwoI* site would cut the 530-bp amplicon into 2 fragments of ~190 bp and 1 fragment of 144 bp. Digestion of uncorrected clone amplicons lead to bands of 336 and 194 bp. (D) The corrected sequence and the silent mutation in the serine codon were detected via Sanger sequencing. (E) The 2 healthy isogenic cell lines and the positive control NB-4 cells expressed HAX1 protein analyzed by western blotting. HAX1^{W44X}-iPSCs showed no HAX1 expression. (F) Normal karyotype with no chromosomal aberrations could be detected in HAX1^{corrected}-iPSCs.

were well-characterized regulators of granulocyte differentiation, such as the lineage-determining transcription factor PU.1.³³ These findings suggest perturbation of the granulocytic differentiation program already at the progenitor cell stage. Correction of mutated

HAX1 in isogenic HAX1^{corrected}-iPSCs led to a complete reversal of the perturbed expression (Figure 4B-C; supplemental Figure 6B-C; supplemental Table 4), providing molecular proof for the rescue of granulocytic differentiation.

Figure 3. Neutrophilic in vitro differentiation showed recapitulation of Kostmann phenotype and rescue upon genetic correction.

(A) Schematic overview of the hematopoietic in vitro differentiation protocol. Spin-EBs were generated, selected, and transferred into plates for adhesion. Attached EBs formed myeloid cell-forming complexes that released progenitors as suspension cells into the medium. After hematopoietic specification, step suspension cells were collected and applied to neutrophilic differentiation. IL-3, interleukin-3. (B-C) After neutrophilic differentiation, morphology was assessed by (B) May-Grünwald Giemsa staining of cytopsins. Original magnification $\times 200$ (insets, $\times 400$). (C) Percentages of neutrophilic granulocytes (Gran), promyelocytes (Prom) and monocytes (Mono) are presented as mean \pm standard deviation (SD) of $n = 10$ independent experiments. (D) Percentage (mean \pm SD) of $CD15^+$ (neutrophilic marker) $HAX1^{WT/WT}$, $HAX1^{W44X}$, and $HAX1^{corrected}$ cells after neutrophilic differentiation as assessed by flow cytometry ($n = 4$). (E) Representative fluorescence-activated cell sorted plots and gating strategy are shown. The values indicate mean \pm SD of $n = 4$ experiments. (F) DNA staining after PMA stimulation showed NET formation in peripheral blood granulocytes, $HAX1^{WT/WT}$ and $HAX1^{corrected}$ -iPSC-derived cells. Original magnification $\times 100$ (insets, $\times 400$); SYTOX Green stain. (C-D) $**P < .01$ when compared with $HAX1^{W44X}$ -iPSCs.



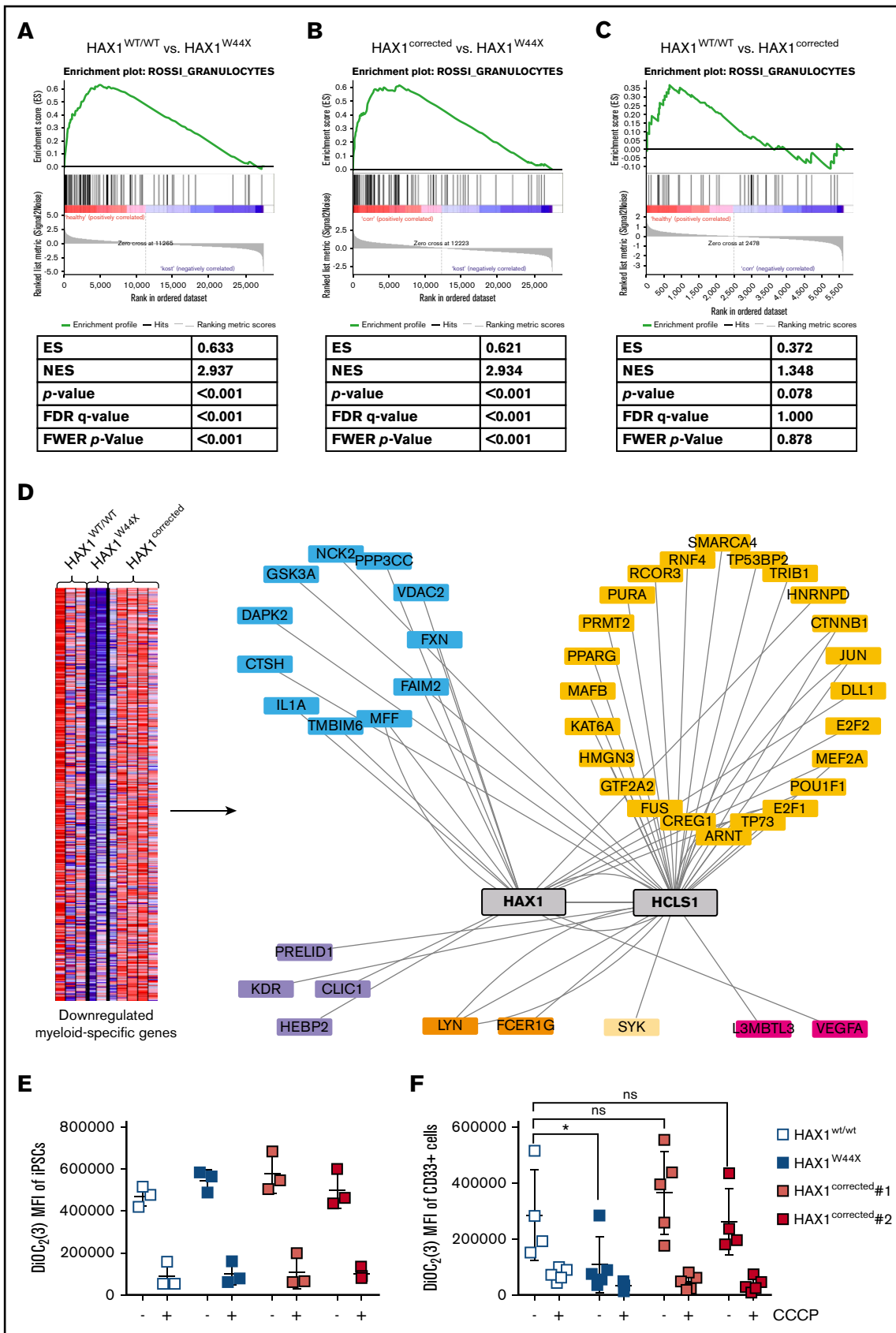


Figure 4.

To understand the cellular processes that are affected by the *HAX1* mutation during granulocytic differentiation, we performed network analysis of the genes specifically downregulated in the *HAX1*^{W44X} samples (supplemental Figures 7 and 8; for quantitative RT-PCR validation of selected genes, see supplemental Figure 9A). We observed that the downregulated genes are strongly interconnected by various known and predicted direct protein-protein interactions (Figure 4D; supplemental Figure 9B). The network analysis revealed nodes or clusters of interactions that could be attributed to gene ontology (GO) categories related to mitochondrial homeostasis (apoptotic mitochondrial changes, regulation of mitochondrial membrane potential) and the activation of apoptotic signaling pathways (regulation of apoptotic signaling pathway, regulation of leukocytic apoptosis, apoptotic mitochondrial changes). Accordingly, the mitochondrial membrane potential of *HAX1*^{W44X} CD33⁺ myeloid progenitors but not of *HAX1*^{W44X}-iPSCs is lower compared with the respective isogenic *HAX1*^{corrected} or *HAX1*^{WT/WT} samples (Figure 4E-F). This translates into a higher rate of apoptosis in *HAX1*^{W44X} myeloid progenitors (supplemental Figure 10). However, the deregulation of clusters of genes involved in transcriptional control, myeloid cell behavior and reactive oxygen metabolism (GO terms: transcription factor binding, granulocytic migration, myeloid cell homeostasis, and reactive oxygen species [ROS] metabolic process) indicates functions of *HAX1* beyond mitochondrial apoptosis. Inversely, the respective GO sets (containing all genes of the respective GO category) were negatively enriched in *HAX1*^{W44X} samples confirming their regulation by *HAX1*. Most important, the interaction network of downregulated genes is centered around *HAX1* and *HCLS1* and includes several direct interaction partners of either protein (Figure 4D; supplemental Figure 9A-B). For example, the interaction of *GSK3A* and *HCLS1* has been experimentally validated.³⁴ *GSK3A* is a crucial player in Wnt signaling and interacts with *CTNNB1/LEF1* as well as *JUN*.³⁵ *CTNNB1* is also among the downregulated genes in *HAX1*^{W44X} myeloid progenitors. *TMBIM6* is an inhibitor of *BAX1*-induced apoptosis and is directly related to the function of *HAX1* in preventing mitochondrial outer membrane permeabilization by *BAX* accumulation.³⁶ Central for this function of *HAX1* is *PARL*,⁹ which is 1 of the downregulated genes in the *HAX1*^{W44X}-iPSC-derived granulocytic progenitors.

Thus, mutation of *HAX1* leads to global changes in transcription networks involved in the regulation of apoptosis and myeloid differentiation. Correction of mutated *HAX1* reverses those changes, reestablishing normal myeloid cell homeostasis and differentiation.

Discussion

Here we demonstrate the successful establishment of an iPSC model for Kostmann disease that recapitulates the granulocytic differentiation arrest and compensatory monocyte overproduction

seen in patients. We showed that targeted genetic correction of the *HAX1* mutation reestablished a *HAX1*- and *HCLS1*-centered transcription network in immature myeloid progenitors, which is not only involved in the regulation of apoptosis, but also myeloid differentiation. Our study demonstrates that correction of the underlying genetic event in Kostmann patients using the CRISPR-Cas9 system might be used as a therapeutic intervention to cure the disease in the affected patients without causing genotoxicity introduced by virus-based strategies.^{37,38}

Virus-based gene transfer has been successfully applied in current gene therapy trials^{39,40}; however, viral gene therapy harbors the risk of inducing hematologic malignancies or, on the other hand, treatment failure resulting from silencing of the transgene.^{37,41-43} Transgene silencing is a particular problem upon use of lentivirally transduced iPSCs to derive hematologic cells.⁴⁴⁻⁴⁶ During the differentiation process, the open chromatin of iPSCs undergoes complex epigenomic changes,⁴⁷ which can hamper transgene expression.⁴⁸ In our hands, a rescue approach for the hematopoietic differentiation arrest of *HAX1*^{W44X}-iPSCs by lentiviral overexpression of WT codon-optimized *HAX1* cDNA was unsuccessful (supplemental Figure 11A-D). Even for disease-modeling approaches, the use of lentiviral-based cDNA overexpression for the correction of the respective disease phenotype is imprecise because of potentially occurring insertional mutagenesis and unknown effects of constitutively high transgene expression using viral promoters in cells, which normally do not express the protein.⁴⁹ This can lead to a defective activation of cellular processes, which has also been observed in clinical trials for X-linked chronic granulomatous disease. Here, the overexpression of *CYBB* (gp90^{phox}), a subunit of the reduced NAD phosphate oxidase enzyme complex, impaired long-term engraftment of HSCs after transplantation⁵⁰ resulting from improper ROS production.⁵¹

The use of gene-editing techniques circumvents several of these issues. By precise genetic correction of the “disease-causing” mutation in patient-derived iPSCs, isogenic cell lines were derived that differ from the parental iPSC line only by the targeted sequence. This provides optimal experimental conditions for iPSC disease modeling as patient-specific or clonal variability between different iPSC lines can be largely excluded.^{52,53} Furthermore, this strategy allows for confidence in genetic causality without the necessity of animal models.⁵⁴⁻⁵⁶ Our CRISPR-Cas9- and homology-directed repair-based 1-step cell transfection and screening protocol allowed the generation and identification of corrected clones in less than 3 weeks with no detectable chromosomal aberrations or mutations at the sgRNA's top predicted 5 off-target sites. Although whole genome sequencing is required to fully exclude off-target cleavage of the Cas9 endonuclease,⁵⁷⁻⁵⁹ careful selection of the sgRNAs and the subsequent data indicate that our system provides genetically

Figure 4. Expression profiling of iPSC-derived CD33⁺ myeloid progenitors identified a downregulated genetic interaction network in Kostmann disease. The granulocyte-specific gene set is positively enriched in (A) *HAX1*^{WT/WT} and (B) *HAX1*^{corrected} myeloid progenitors compared with *HAX1*^{W44X} cells. (C) When comparing *HAX1*^{WT/WT} and *HAX1*^{corrected} cells, no significant enrichment could be observed, suggesting that those groups show similar granulocytic expression patterns. ES, enrichment score; FDR, false discovery rate; FWER, family-wise error rate; NES, normalized enrichment score. (D) Heatmap (left) of the 533 myeloid-specific genes (leading edge subsets) that were downregulated in *HAX1*^{W44X}-iPSC-derived myeloid progenitors as compared with *HAX1*^{WT/WT}- and *HAX1*^{corrected}-iPSC-derived cells. Those were used to form a gene interaction network (supplemental Figure 9B). The downregulated gene interaction partners of *HAX1* and *HCLS1* in *HAX1*^{W44X}-iPSC-derived CD33⁺ granulocytic progenitors are shown (right). (E-F) 3,3'-diethylthiocarbocyanine iodide (DiOC₂(3)) mean fluorescence intensity (MFI) of (E) TRA-1-60⁺ iPSCs and (F) CD33⁺ cells during induced myeloid differentiation with or without addition of mitochondrial membrane potential disruptor carbonyl cyanide 3-chlorophenylhydrazone (CCCP). Mean ± SD of n = 4-5 experiments are shown. NS, not significant. *P < .05 when compared with *HAX1*^{wt/wt}.

defined conditions to investigate the net effect of the *HAX1*^{W44X} mutation, as it was previously shown for *ELANE* mutations in SCN and X-linked chronic granulomatous disease.^{60,61} These isogenic iPSCs can facilitate drug or toxicity screenings to find the most advantageous therapies in this rare disease; furthermore, they create an ideal platform for the development of improved therapy in SCN.

HAX1 is primarily located in the mitochondrial membrane, endoplasmic reticulum, and cytoplasm.⁶⁻⁸ Since the identification of *HAX1* mutations in Kostmann disease, it remained unclear why patients show selectively impaired neutrophilic differentiation. By genome-wide expression profiling of iPSC-derived isogenic myeloid progenitor cells, we demonstrate that the *HAX1*^{W44X} mutation not only affects the expression of genes involved in apoptosis or apoptotic mitochondrial changes, but also impaired expression of central transcriptional regulators of myeloid differentiation. Among the differentially repressed genes in the *HAX1*^{W44X}-iPSC-derived myeloid progenitors was *HCLS1*, which is the direct interaction partner of *HAX1*.⁶ Skokowa et al highlighted the essential role of G-CSF-mediated *HCLS1* activation and nuclear translocation via association of the Lyn and Syk kinases during granulopoiesis.¹⁰ In agreement with this observation, our findings demonstrate that this important axis for granulocytic differentiation was downregulated in *HAX1*^{W44X}-iPSC-derived cells (Figure 4D). Similarly, the expression of key members of the Wnt-signaling cascade (*GSK3A* and *CTNNB1*) that is a crucial player in the pathogenesis of SCN,¹⁰ was affected by the *HAX1* mutation. Interestingly, these observations also support previous findings that the SCN phenotype can be partially rescued in vitro by addition of Wnt3a.⁶² Noteworthy is that, by using purified myeloid progenitor cells, these defects already affect the specification process: an observation only feasible because of the generation of a fully isogenic-iPSC amendable to interrogate all stages of Kostmann disease. Furthermore, *HAX1* appears to carry out antiapoptotic functions through the inhibition of MOMP by PARL-mediated activation of *HTRA2*.⁹ Recently, Abdelwahid et al demonstrated *HAX1*-mediated cell survival by protection from multiple apoptotic signals in a cardiomyocyte cell line.⁶³ We also observed deregulation of genes involved in a multitude of apoptotic processes, such as *PARL*, *FAM2*, and *TMBIM6*, suggesting that the role of *HAX1* and *HCLS1* in apoptosis of myeloid cells may be another key function in the Kostmann disease genetic network. In fact, we validated decreased mitochondrial membrane potential and increased apoptosis in those cells. Moreover, enhanced ROS production and subsequent DNA damage have been suggested to play a major role in the acquisition of neutropenia phenotype of Barth syndrome.⁶⁴ We also identified downregulated genes in ROS metabolism, including *CYBB*, *NCF1*, and *NCF2*, which are mutated in chronic granulomatous disease.⁶⁵⁻⁶⁷ Together with other important neutrophilic genes such as *MPO*, *NOX4*, and *SOD2*, the ROS metabolism seems to be 1 of the central processes impaired in the myeloid cell differentiation of *HAX1*^{W44X}-iPSCs.

Here we have demonstrated that targeted genetic correction of the *HAX1* gene is applicable to repair patient-derived iPSCs. Moreover,

we showed that the neutropenia phenotype observed upon in vitro differentiation could be reversed in corrected iPSCs, and we were able to demonstrate that monocytosis observed in patients⁵ is also recapitulated in culture. Taken together, we show that the iPSC differentiation system is suitable for study of the clinical phenotype of Kostmann SCN and to develop new therapeutic options. In addition, we suggest a Kostmann disease-specific gene signature in which *HAX1* and *HCLS1* act as the central players of a large dysregulated genetic network and that suggest further implications of *HAX1* to other important cellular signaling pathways.

Acknowledgments

The authors thank M. Ballmaier for cell sorting, and K. Weber and B. Fehse for providing LeGO plasmids.

This work was supported by grants to J.-H.K. and T.C. from the José Carreras Leukemia Foundation. J.-H.K. is a fellow of the Emmy Noether-Programme of the German Research Foundation (DFG) (KL-2374/2-1). N.L. was supported by the DFG (LA 3680/2-1), the Else Kröner-Fresenius-Stiftung (2015_A92), and Hannover Medical School (young academy program). E.P. was supported by the Hannover Biomedical Research School. D.H. was supported by the Max-Eder program from the German Cancer Aid (no. 111743). A.S., G.G., N.L., E.P., and T.C. were supported by the DFG (Cluster of Excellence REBIRTH EXC 62/3 and/or SFB738). G.M. and S.H.O. were supported in part by National Institutes of Health, National Heart, Lung, and Blood Institute U01 HL100001 (Human Pluripotent Stem Cell and Progenitor Models of Cardiac and Blood Diseases, G. Q. Daley, principal investigator).

Authorship

Contribution: E.P. conducted all experiments, analyzed the data, and wrote the manuscript; J.-H.K. designed and supervised the project, planned the experiments, analyzed the data, and wrote the manuscript; T.C. designed and supervised the project and revised the manuscript; A.S. provided *OCT4*, *KLF4*, and *SOX2* and codon-optimized *HAX1* complementary DNA vectors, and cosupervised the project; D.H. designed experiments and revised the manuscript; S.E., M.A., and N.L. provided technical assistance and analyzed the data; G.M. and S.H.O. designed experiments, interpreted data, and revised the manuscript; G.G. and B.S. performed the cytogenetic analysis and interpreted the data; and K.W., codirector of the Severe Chronic Neutropenia International Registries, provided the human Kostmann disease sample and revised the manuscript.

Conflict-of-interest disclosure: The authors declare no competing financial interests.

ORCID profiles: J.-H.K., 0000-0002-1070-0727.

Correspondence: Jan-Henning Klusmann, Department of Pediatric Hematology and Oncology, Hannover Medical School, Carl-Neuberg-Str 1, D-30625 Hannover, Germany; e-mail: klusmann.jan-henning@mh-hannover.de.

References

1. Welte K, Zeidler C, Dale DC. Severe congenital neutropenia. *Semin Hematol*. 2006;43(3):189-195.
2. Kostmann R. Infantile genetic agranulocytosis; agranulocytosis infantilis hereditaria. *Acta Paediatr Suppl*. 1956;45(Suppl 105):1-78.
3. Boztug K, Klein C. Novel genetic etiologies of severe congenital neutropenia. *Curr Opin Immunol*. 2009;21(5):472-480.

4. Roques G, Munzer M, Barthez MA, et al. Neurological findings and genetic alterations in patients with Kostmann syndrome and HAX1 mutations. *Pediatr Blood Cancer*. 2014;61(6):1041-1048.
5. Klein C, Grudzien M, Appaswamy G, et al. HAX1 deficiency causes autosomal recessive severe congenital neutropenia (Kostmann disease). *Nat Genet*. 2007;39(1):86-92.
6. Suzuki Y, Demoliere C, Kitamura D, Takeshita H, Deuschle U, Watanabe T. HAX-1, a novel intracellular protein, localized on mitochondria, directly associates with HS1, a substrate of Src family tyrosine kinases. *J Immunol*. 1997;158(6):2736-2744.
7. Vafiadaki E, Arvanitis DA, Pagakis SN, et al. The anti-apoptotic protein HAX-1 interacts with SERCA2 and regulates its protein levels to promote cell survival. *Mol Biol Cell*. 2009;20(1):306-318.
8. Grzybowska EA, Zayat V, Konopiński R, et al. HAX-1 is a nucleocytoplasmic shuttling protein with a possible role in mRNA processing. *FEBS J*. 2013;280(1):256-272.
9. Chao JR, Parganas E, Boyd K, Hong CY, Opferman JT, Ihle JN. Hax1-mediated processing of HtrA2 by Parl allows survival of lymphocytes and neurons. *Nature*. 2008;452(7183):98-102.
10. Skokowa J, Klimiankou M, Klimenkova O, et al. Interactions among HCLS1, HAX1 and LEF-1 proteins are essential for G-CSF-triggered granulopoiesis. *Nat Med*. 2012;18(10):1550-1559.
11. Peckl-Schmid D, Wolkerstorfer S, Königsberger S, et al. HAX1 deficiency: impact on lymphopoiesis and B-cell development. *Eur J Immunol*. 2010;40(11):3161-3172.
12. Groß B, Pittermann E, Reinhardt D, Cantz T, Klusmann JH. Prospects and challenges of reprogrammed cells in hematology and oncology. *Pediatr Hematol Oncol*. 2012;29(6):507-528.
13. Mucci A, Kunkiel J, Suzuki T, et al. Murine iPSC-derived macrophages as a tool for disease modeling of hereditary pulmonary alveolar proteinosis due to Csf2rb deficiency. *Stem Cell Rep*. 2016;7(2):292-305.
14. Müller LU, Schlaeger TM, DeVine AL, Williams DA. Induced pluripotent stem cells as a tool for gaining new insights into Fanconi anemia. *Cell Cycle*. 2012;11(16):2985-2990.
15. Pomp O, Colman A. Disease modelling using induced pluripotent stem cells: status and prospects. *BioEssays*. 2013;35(3):271-280.
16. Morishima T, Watanabe K, Niwa A, et al. Genetic correction of HAX1 in induced pluripotent stem cells from a patient with severe congenital neutropenia improves defective granulopoiesis. *Haematologica*. 2014;99(1):19-27.
17. Germeshausen M, Grudzien M, Zeidler C, et al. Novel HAX1 mutations in patients with severe congenital neutropenia reveal isoform-dependent genotype-phenotype associations. *Blood*. 2008;111(10):4954-4957.
18. Lachmann N, Ackermann M, Frenzel E, et al. Large-scale hematopoietic differentiation of human induced pluripotent stem cells provides granulocytes or macrophages for cell replacement therapies. *Stem Cell Rep*. 2015;4(2):282-296.
19. Warlich E, Kuehle J, Cantz T, et al. Lentiviral vector design and imaging approaches to visualize the early stages of cellular reprogramming. *Mol Ther*. 2011;19(4):782-789.
20. Weber K, Bartsch U, Stocking C, Fehse B. A multicolor panel of novel lentiviral "gene ontology" (LeGO) vectors for functional gene analysis. *Mol Ther*. 2008;16(4):698-706.
21. Ran FA, Hsu PD, Wright J, Agarwala V, Scott DA, Zhang F. Genome engineering using the CRISPR-Cas9 system. *Nat Protoc*. 2013;8(11):2281-2308.
22. Cong L, Ran FA, Cox D, et al. Multiplex genome engineering using CRISPR/Cas systems. *Science*. 2013;339(6121):819-823.
23. Heckl D, Kowalczyk MS, Yudovich D, et al. Generation of mouse models of myeloid malignancy with combinatorial genetic lesions using CRISPR-Cas9 genome editing. *Nat Biotechnol*. 2014;32(9):941-946.
24. Subramanian A, Tamayo P, Mootha VK, et al. Gene set enrichment analysis: a knowledge-based approach for interpreting genome-wide expression profiles. *Proc Natl Acad Sci USA*. 2005;102(43):15545-15550.
25. Reimand J, Arak T, Adler P, et al. g:Profiler—a web server for functional interpretation of gene lists (2016 update). *Nucleic Acids Res*. 2016;44(W1):W83-W89.
26. Warde-Farley D, Donaldson SL, Comes O, et al. The GeneMANIA prediction server: biological network integration for gene prioritization and predicting gene function. *Nucleic Acids Res*. 2010;38(web server issue):W214-W220.
27. Shannon P, Markiel A, Ozier O, et al. Cytoscape: a software environment for integrated models of biomolecular interaction networks. *Genome Res*. 2003;13(11):2498-2504.
28. Bock C, Kiskinis E, Verstappen G, et al. Reference maps of human ES and iPS cell variation enable high-throughput characterization of pluripotent cell lines. *Cell*. 2011;144(3):439-452.
29. Yang L, Guell M, Byrne S, et al. Optimization of scarless human stem cell genome editing. *Nucleic Acids Res*. 2013;41(19):9049-9061.
30. CRISPR design tool. <http://crispr.mit.edu/>.
31. Gazit R, Mandal PK, Ebina W, et al. Fgd5 identifies hematopoietic stem cells in the murine bone marrow. *J Exp Med*. 2014;211(7):1315-1331.
32. Novershtern N, Subramanian A, Lawton LN, et al. Densely interconnected transcriptional circuits control cell states in human hematopoiesis. *Cell*. 2011;144(2):296-309.
33. Anderson KL, Smith KA, Pio F, Torbett BE, Maki RA. Neutrophils deficient in PU.1 do not terminally differentiate or become functionally competent. *Blood*. 1998;92(5):1576-1585.

34. Lin A, Wang RT, Ahn S, Park CC, Smith DJ. A genome-wide map of human genetic interactions inferred from radiation hybrid genotypes. *Genome Res.* 2010;20(8):1122-1132.
35. Wei W, Jin J, Schlisio S, Harper JW, Kaelin WG Jr. The v-Jun point mutation allows c-Jun to escape GSK3-dependent recognition and destruction by the Fbw7 ubiquitin ligase. *Cancer Cell.* 2005;8(1):25-33.
36. Xu Q, Reed JC. Bax inhibitor-1, a mammalian apoptosis suppressor identified by functional screening in yeast. *Mol Cell.* 1998;1(3):337-346.
37. Hacein-Bey-Abina S, Von Kalle C, Schmidt M, et al. LMO2-associated clonal T cell proliferation in two patients after gene therapy for SCID-X1. *Science.* 2003;302(5644):415-419.
38. Cesana D, Ranzani M, Volpin M, et al. Uncovering and dissecting the genotoxicity of self-inactivating lentiviral vectors in vivo. *Mol Ther.* 2014;22(4):774-785.
39. Aiuti A, Biasco L, Scaramuzza S, et al. Lentiviral hematopoietic stem cell gene therapy in patients with Wiskott-Aldrich syndrome. *Science.* 2013;341(6148):1233151.
40. Biffi A, Montini E, Lorioli L, et al. Lentiviral hematopoietic stem cell gene therapy benefits metachromatic leukodystrophy. *Science.* 2013;341(6148):1233158.
41. Baum C. Gene therapy for SCID-X1: focus on clinical data. *Mol Ther.* 2011;19(12):2103-2104.
42. Stein S, Ott MG, Schultze-Strasser S, et al. Genomic instability and myelodysplasia with monosomy 7 consequent to EVI1 activation after gene therapy for chronic granulomatous disease. *Nat Med.* 2010;16(2):198-204.
43. Ackermann M, Lachmann N, Hartung S, et al. Promoter and lineage independent anti-silencing activity of the A2 ubiquitous chromatin opening element for optimized human pluripotent stem cell-based gene therapy. *Biomaterials.* 2014;35(5):1531-1542.
44. Mukherjee S, Santilli G, Blundell MP, Navarro S, Bueren JA, Thrasher AJ. Generation of functional neutrophils from a mouse model of X-linked chronic granulomatous disorder using induced pluripotent stem cells. *PLoS One.* 2011;6(3):e17565.
45. Raya A, Rodriguez-Pizà I, Guenechea G, et al. Disease-corrected haematopoietic progenitors from Fanconi anaemia induced pluripotent stem cells. *Nature.* 2009;460(7251):53-59.
46. Minoguchi S, Iba H. Instability of retroviral DNA methylation in embryonic stem cells. *Stem Cells.* 2008;26(5):1166-1173.
47. Hawkins RD, Hon GC, Lee LK, et al. Distinct epigenomic landscapes of pluripotent and lineage-committed human cells. *Cell Stem Cell.* 2010;6(5):479-491.
48. Herbst F, Ball CR, Tuorto F, et al. Extensive methylation of promoter sequences silences lentiviral transgene expression during stem cell differentiation in vivo. *Mol Ther.* 2012;20(5):1014-1021.
49. Thomas CE, Ehrhardt A, Kay MA. Progress and problems with the use of viral vectors for gene therapy. *Nat Rev Genet.* 2003;4(5):346-358.
50. Kang HJ, Bartholomae CC, Paruzynski A, et al. Retroviral gene therapy for X-linked chronic granulomatous disease: results from phase I/II trial. *Mol Ther.* 2011;19(11):2092-2101.
51. Grez M, Reichenbach J, Schwäble J, Seger R, Dinauer MC, Thrasher AJ. Gene therapy of chronic granulomatous disease: the engraftment dilemma. *Mol Ther.* 2011;19(1):28-35.
52. Onder TT, Daley GO. New lessons learned from disease modeling with induced pluripotent stem cells. *Curr Opin Genet Dev.* 2012;22(5):500-508.
53. Kim HS, Bernitz JM, Lee DF, Lemischka IR. Genomic editing tools to model human diseases with isogenic pluripotent stem cells. *Stem Cells Dev.* 2014;23(22):2673-2686.
54. Yusa K, Rashid ST, Strick-Marchand H, et al. Targeted gene correction of α 1-antitrypsin deficiency in induced pluripotent stem cells. *Nature.* 2011;478(7369):391-394.
55. Sanders LH, Laganière J, Cooper O, et al. LRRK2 mutations cause mitochondrial DNA damage in iPSC-derived neural cells from Parkinson's disease patients: reversal by gene correction. *Neurobiol Dis.* 2014;62:381-386.
56. Sebastiano V, Maeder ML, Angstman JF, et al. In situ genetic correction of the sickle cell anemia mutation in human induced pluripotent stem cells using engineered zinc finger nucleases. *Stem Cells.* 2011;29(11):1717-1726.
57. Hsu PD, Scott DA, Weinstein JA, et al. DNA targeting specificity of RNA-guided Cas9 nucleases. *Nat Biotechnol.* 2013;31(9):827-832.
58. Fu Y, Foden JA, Khayter C, et al. High-frequency off-target mutagenesis induced by CRISPR-Cas nucleases in human cells. *Nat Biotechnol.* 2013;31(9):822-826.
59. Cho SW, Kim S, Kim Y, et al. Analysis of off-target effects of CRISPR/Cas-derived RNA-guided endonucleases and nickases. *Genome Res.* 2014;24(1):132-141.
60. Nayak RC, Trump LR, Aronow BJ, et al. Pathogenesis of ELANE-mutant severe neutropenia revealed by induced pluripotent stem cells. *J Clin Invest.* 2015;125(8):3103-3116.
61. Merling RK, Kuhns DB, Sweeney CL, et al. Gene-edited pseudogene resurrection corrects p47phox-deficient chronic granulomatous disease. *Blood Adv.* 2017;1:270-278.
62. Hiramoto T, Ebihara Y, Mizoguchi Y, et al. Wnt3a stimulates maturation of impaired neutrophils developed from severe congenital neutropenia patient-derived pluripotent stem cells. *Proc Natl Acad Sci USA.* 2013;110(8):3023-3028.
63. Abdelwahid E, Li H, Wu J, Irioda AC, de Carvalho KA, Luo X. Endoplasmic reticulum (ER) stress triggers Hax1-dependent mitochondrial apoptotic events in cardiac cells. *Apoptosis.* 2016;21(11):1227-1239.

64. van Raam BJ, Kuijpers TW. Mitochondrial defects lie at the basis of neutropenia in Barth syndrome. *Curr Opin Hematol*. 2009;16(1):14-19.
65. Rae J, Newburger PE, Dinayer MC, et al. X-linked chronic granulomatous disease: mutations in the CYBB gene encoding the gp91-phox component of respiratory-burst oxidase. *Am J Hum Genet*. 1998;62(6):1320-1331.
66. Vázquez N, Lehrnbecher T, Chen R, et al. Mutational analysis of patients with p47-phox-deficient chronic granulomatous disease: the significance of recombination events between the p47-phox gene (NCF1) and its highly homologous pseudogenes. *Exp Hematol*. 2001; 29(2):234-243.
67. Roos D, van Buul JD, Tool AT, et al. Two CGD families with a hypomorphic mutation in the activation domain of p67phox. *J Clin Cell Immunol*. 2014;5(3): 1000231.